Local Mass Transfer and Skin Friction from a Sphere using Electrochemical Probes," Letters in Heat Mass Transfer, **2**, 247 (1975).
Gostkowski, V. J., and F. A. Costello, "The Effect of Free Stream Turbulence on Heat Transfer from the Stagnation Point of a Sphere," *Int. J. Heat Mass Transfer*, **13**, 1382 (1970).
Hinze, J. D., *Turbulence* 2nd ed. McGraw Hill Book Co., New York (1975).
Hsu, N. T., and B. H. Sage, "Thermal and Material Transfer in Turbulent Gas Streams: Local Transport from Spheres," *AIChE J.*, **3**, 405 (1957).
Kestin, J., and R. T. Wood, "The Influence of Turbulence on Mass Transfer from Cylinders," *J. Heat Transfer*, **93**, 321 (1971).
Kolmogoroff, A. N., *On Degeneration of Isotropic Turbulence in an Incompressible Viscous Liquid*, C. R. Akad. Nauk. S.S.S.R., **31**, 538 (1941).
Lavender, W.I., and D. C. T. Pei, "The Effect of Fluid Turbulence on the Rate of Heat Transfer from Spheres," *Int. J. Heat Mass Transfer*, **10**, 529 (1967).
Maisel, D. S., and T. K. Sherwood, "Effect of Air Turbulence on Rate of Evaporation of Water," *Chem. Eng. Prog.*, **46**, 131 (1950).
Mizushina, T., "Electrochemical Method in Transport Phenomena," *Advances in Heat Transfer*, p. 87, **7**, Academic Press, New York, London (1970).
Raithby, G. D., and E. R. G. Eckert, "The Effect of Turbulence Parameters and Support Position on the Heat Transfer from Spheres," *Int. J. Heat Mass Transfer*, **11**, 1233 (1968).
Sandoval, J. G., "Transfert de Matière entre une Sphère Solide et un Liquide. Influence de la Turbulence," *Thèse Doc. Ing.*, Inst. Nat. Polytech., Toulouse (1978).
Sandoval, J. G., J. P. Riba and J. P. Couderc, "Mass Transfer around a Sphere," *Trans. Inst. Chem. Eng.*, **58**, 132 (1980).
Smith, M. C., and A. M. Kuethe, "Effects of Turbulence on Laminar Skin Friction and Heat Transfer," *Phys. Fluids*, **9**, 2337 (1966).
Venezian, E., M. J. Crespo and B. H. Sage, "Thermal and Material Transfer in Turbulent Gas Streams: One inch Spheres," *AIChE J.*, **8**, 383 (1962).
Yuge, T., "Experiments on Heat Transfer of Spheres, Including Combined Natural and Forced Convection," *J. Heat Transfer*, **82**, 214 (1960).

Manuscript received October 5, 1979; revision received May 2, and accepted December 10, 1980.

Revision of Kynch Sedimentation Theory

FRANK M. TILLER

M. D. Anderson Professor of Chemical Engineering
University of Houston
Houston, TX 77004

Much of the theory of gravity sedimentation has been based on the work of Coe and Clevenger (1916) and Kynch (1952). They provided methods for obtaining rates of sedimentation in batch, static tests which are presently used for design of continuous thickeners. Kynch assumed that a first order partial differential equation controlled the entire sedimentation process. His equation was based on: (1) continuity balance; and (2) sedimentation velocity being a unique function of solid particulate concentration. A general solution was presented in the form of volume fraction of solids $\phi_s = f(x - vt)$. During the constant rate fall of the upper interface, the boundary condition of uniform initial concentration combines with the Kynch equations to adequately describe the sedimentation phenomena. Kynch ignored the sediment rising from the bottom of the settling chamber, and assumed that the characteristics $y = x - vt$ originated at the origin of coordinates (height, time) during the first falling rate period. The characteristics actually originate at the surface of the rising sediment where the upward liquid velocity affects the rate of fall of the particulates. New equations have been derived based upon the assumption that the characteristics emanate from the rising sediment.

SCOPE

Gravity sedimentation is used to thicken slurries prior to filtration or centrifugation. Normally a larger fraction of the total liquid is removed in thickening than in subsequent operations. Continuous thickeners involve a clear zone of small turbidity, a region of line settling of particles, and a sediment zone. In the clear zone, individual particles rise or fall in a Stokesian regime. Under ideal conditions, particles in line or hindered settling have uniform velocities independent of particle size distribution. The sediment or compression zone involves a structural network of particles capable of sustaining compressive forces. The particulate structure has a low yield stress and compresses readily under the weight of the buoyed particles. The compressive or effective pressure due to the sediment weight increases with depth leading to a decrease in porosity.

0001-1541-81-4908-0823-$2.00.

Motion of rakes, introduction of feed in a center feedwell, and methods of removal of the overflow and underflow contribute to three-dimensional flow patterns which complicate actual behavior of industrial thickeners.

For many years, design of gravity thickeners has been based upon the work of Coe and Clevenger (1916), and Kynch (1952) as modified by Talmadge and Fitch (1955) and discussed at length by Scott (1966, 1968) and Fitch (1966, 1977). The Kynch procedure is appealing because it permits the velocity of sedimentation u_s and the volumetric flux/area, $F = u_s\phi_s$ to be determined as functions of a range of volumetric fraction of solids ϕ_s in a single run. The Coe and Clevenger method requires preparation of slurries of different concentration whose rates of sedimentation are determined separately thus requiring more time and possibly larger samples than with the Kynch technique. In addition when flocculants are used, the Kynch procedure is attractive because time is diminished and

less handling and agitation of the suspension are required.

For mathematical purposes, batch sedimentation can be divided into three zones depending upon the position of the upper and lower phase boundaries. These are generally called the constant rate, first, and second falling rate zones. The constant rate zone ends when the upper phase boundary ceases to fall linearly. The end is marked by the intersection of a characteristic emanating from the initial layer of sediment and the locus of the upper phase boundary. The first falling rate period ends when the upper and lower phase boundaries merge. At that point, all of the particles are incorporated in the compressible sediment. The second falling rate period involves squeezing of liquid out of the sediment under the force of the buoyed weight of solids.

A nonlinear, second-order, partial differential equation of Darcy type governs the flow of liquid out of the sediments whereas a first-order partial differential equation is applicable to the sedimenting zone. In the first falling rate period, boundary conditions for the first and second order equations must be matched at the surface of the rising sediment.

The Kynch procedure applies exactly only to the first stage which is of a somewhat trivial nature as the suspension concentration remains constant. To an unknown degree, his equations approximate the second stage but should not be used in the third or compression zone.

The proposed equations are based upon knowing heights of upper and lower phase boundaries as a function of time. A graphical procedure similar to one developed in connection with the Kynch procedure has been developed. If the sediment height is assumed to be zero (infinite sediment density) at all times, the proposed procedure reduces to the Kynch method as commonly used.

CONCLUSIONS AND SIGNIFICANCE

A few studies (Scott and Alderton, 1966) have been undertaken to compare different design methods. Although the Coe and Clevenger method should yield the same results as the Kynch method, actual calculations have shown discrepancies. Inasmuch as calculations were based upon an assumed correctness of Kynch mathematics, it is probable that errors were involved. Methods proposed in this paper provide a means for improving calculations.

The equations as presented are of an implicit type and do not offer a simple straightforward way of obtaining flux curves as developed on the basis of Kynch mathematics. They do offer a means for testing consistency of data. Further investigation may yield useful simplification.

INTRODUCTION

Batch laboratory sedimentation experiments are frequently carried out in one or two liter graduated cylinders. Most data reported in the literature refer only to the descending upper phase boundary and omit the equally important rising sediment. A typical sedimentation process is illustrated in Figure 1. The upper interface is represented by H vs. t and the sediment by L vs. t. In the constant rate period, H is linear in t. A characteristic represented by the dotted line emanates from the origin and intersects the H vs. t locus at A at the end of the constant rate period. The first falling rate period is caused by upward movement of liquid as it is squeezed out of the sediment. The rate at which liquid is expressed from the compacting solids fixes the upward fluid velocity at the sediment-suspension interface. As the sediment grows in thickness and liquid is squeezed out at an increasing rate, characteristics leave the sediment surface and pass up through the sedimenting particulates. Those characteristics flow along lines of constant composition and serve as signals for the suspension to settle more slowly.

When the upper descending boundary meets the ascending sediment at B, the second falling rate period begins. Further decrease in height is effected solely by flow of liquid out of the compaction zone because of the unbalanced buoyed weight of the solid particles. When the cake structure carries the entire weight of particulates, liquid pressure gradients attain a null state; and no further compression occurs.

The Kynch procedure involves fundamental errors as it does not take the rising sediment into proper account. Ignoring the appearance of a bottom sediment, Kynch postulated that sedimentation velocity u_s was a unique function of solid volume fraction ϕ_s and derived a simple first order partial differential equation describing behavior of the settling particulates. Referring to Figure 1 and noting that u_s and dH/dt are negative quantities, the equation of continuity yields

$$\text{SOLID:} \qquad \frac{\partial \phi_s}{\partial t} + \frac{\partial (u_s \phi_s)}{\partial x} = 0 \tag{1}$$

$$\text{LIQUID:} \qquad \frac{\partial \phi}{\partial t} + \frac{\partial (u \phi)}{\partial x} = 0 \tag{2}$$

where the following notation is employed:

	Volumetric Concentrations		Pore and Anti-Pore Velocity	Flux	
	Suspension	Sediment		Suspension	Sediment
Liquid	ϕ	ϵ	u	$q = u\phi$	$u\epsilon$
Solid	ϕ_s	ϵ_s	u_s	$q_s = u_s\phi_s$	$u_s\epsilon_s$

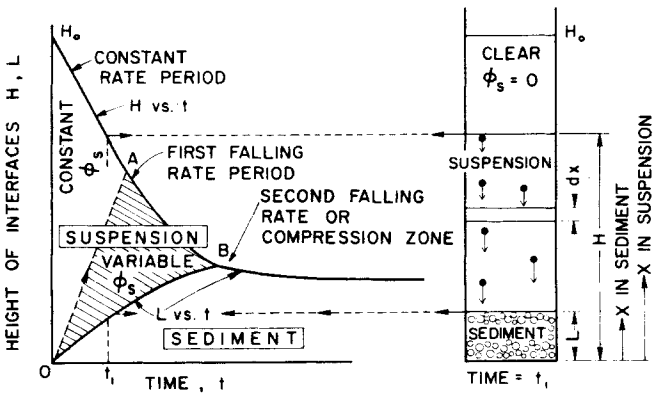

Figure 1. Interfaces in sedimentation.

Inasmuch as Kynch did not concern himself with the sediment, the symbols ϵ and ϵ_s do not appear in his equation. Without direct use of the equation of motion, Kynch combined the assumption that $u_s = f(\phi_s)$ with Eq. 1 as follows:

$$\frac{\partial \phi_s}{\partial t} + \frac{d(u_s\phi_s)}{d\phi_s}\frac{\partial \phi_s}{\partial x} = \frac{\partial \phi_s}{\partial t} + \nu(\phi_s)\frac{\partial \phi_s}{\partial x} = 0 \qquad (3)$$

The solution of this equation is some function of $x - \nu t$ or

$$\phi_s = f(x - \nu t) \qquad (4)$$

When $(x - \nu t)$ is constant, ϕ_s is constant. Along a characteristic line on which

$$x = \nu t + c \qquad (5)$$

the concentration and flux rate will both be constant. Kynch argued incorrectly that c is zero during the falling rate period and that all of the characteristics emanated from the origin. The procedure has also been used for the second falling rate period involving compaction of the sediment. Inasmuch as the laws governing the flow in a compressible sediment differ from the simple equation used for sedimentation, the method cannot be expected to yield correct results during compression.

Data necessary to the solution of both the Kynch and the proposed method are illustrated in Figure 2. The fundamental data needed for the domain of the suspension are shown in Figure 2A in the form of settling velocity u_s vs. suspension concentration. Velocities are shown as negative in accord with notation used herein. When the solution is sufficiently dilute, particles fall independently at different velocities in Stokesian flow; and the methods of this paper are inappropriate to the problem. There is no unique concentration marking a transformation from the Stokes-type region into zone settling. In the very dilute range, suspensions exhibit no sharp line of demarcation between the particulates and the supernatant liquid. The suspension is apt to appear as a cloudy haze.

As concentration increases, an interface begins to form; but considerable turbidity remains in the region above the descending interface. At a sufficiently high concentration, the particles tend to settle in bulk independently of individual sizes. Wide variations are characteristic of the behavior of different slurries. No general discussion of other than simple zone or hindered settling will be undertaken.

Once the concentration has increased sufficiently, the particles enter into mutual contact; and the resulting sediment will be capable of sustaining shear forces without flow. At that point, compaction begins to take place; and the rate of descent of the interface is no longer a function of concentration of the solids at the interface. In fact, the concentration above the interface is then zero. There is no unique velocity or flux curve beyond the critical concentration at which the suspension forms what we shall call a "structure" consisting of interconnected particles. In Figure 2A, the Stokes and sediment compression regions are illustrated for a slow settling attapulgite.

In Figure 2B, the flux curve $F = \phi_s u_s$ is shown as a function of ϕ_s. At point A, the flux is a maximum in the downward direction. Clearly a sediment will have different behavior depending whether it lies to the right or left of A. At point B, the curve has a point of inflection.

The characteristic velocity ν is the slope of the solids flux curve as shown in Figure 2C. The point A transforms into $\nu = 0$; and the inflection point B of Figure 2B becomes the maximum point on Figure 2C.

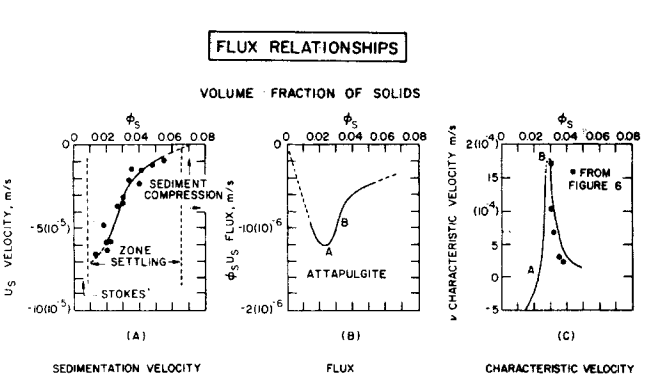

Figure 2. Flux relationships in sedimentation of attapulgite.

EQUATIONS FOR COMPRESSIBLE SEDIMENT

The equations of continuity for the sediment are identical to Eqs. 1 and 2 with ϕ being replaced by ϵ.

$$\text{SOLID:} \qquad \frac{\partial \epsilon_s}{\partial t} + \frac{\partial (u_s\epsilon_s)}{\partial x} = 0 \qquad (6)$$

$$\text{LIQUID:} \qquad \frac{\partial \epsilon}{\partial t} + \frac{\partial (u\epsilon)}{\partial x} = 0 \qquad (7)$$

Adding Eqs. 6 and 7 and noting that $\epsilon + \epsilon_s = 1$ leads to

$$\frac{\partial (u_s\epsilon_s)}{\partial x} + \frac{\partial (u\epsilon)}{\partial x} = 0 \qquad (8a)$$

or

$$\frac{\partial q_s}{\partial x} + \frac{\partial q}{\partial x} = 0 \qquad (8b)$$

where q_s and q are respectively the superficial flow rates of solid and liquid. Integration of this expression at constant t (d'Avila and Sampaio, 1979) yields

$$u_s(1 - \epsilon) + u\epsilon = q_s + q = h(t) \qquad (9)$$

If we assume that the flow (by sedimentation or compression) of particles downward is precisely balanced by the flow of liquid upward, then $h(t) = 0$.

The equation of motion neglecting inertial effects states that the effective pressure on each layer of particles is the result of the downward force of the buoyed weight of the particles minus the upward force of friction due to Darcian flow of the liquid. In differential form, the derivative of the effective pressure p_s is given by

$$\frac{\partial p_s}{\partial x} = -(\rho_s - \rho)g(1 - \epsilon) + \frac{\mu\epsilon}{k}(u - u_s) \qquad (10)$$

where ρ, ρ_s are densities of liquid and solid and k is the permeability. Eliminating u_s by means of Eq. 9 and solving for u yields

$$u = \frac{k(1 - \epsilon)}{\mu\epsilon}\frac{\partial p_s}{\partial x} + \frac{k(1 - \epsilon)^2}{\epsilon}\frac{g(\rho_s - \rho)}{\mu} \qquad (11)$$

Equation 6 is rewritten in the form

$$\frac{d\epsilon}{dp_s}\frac{\partial p_s}{\partial t} + \epsilon\frac{\partial u}{\partial x} + u\frac{d\epsilon}{dp_s}\frac{\partial p_s}{\partial x} = 0 \qquad (12)$$

Equation 11 is substituted in Eq. 12 to yield the final partial differential equation for the sediment, thus

$$\frac{d\epsilon}{dp_s}\frac{\partial p_s}{\partial t} + \frac{k(1 - \epsilon)}{\mu}\frac{\partial^2 p_s}{\partial x^2} + \frac{1}{\mu}\frac{d}{dp_s}[k(1 - \epsilon)]\left(\frac{\partial p_s}{\partial x}\right)^2 + \frac{g\Delta\rho}{\mu}\frac{d}{dp_s}[k(1 - \epsilon)^2]\frac{\partial p_s}{\partial x} = 0 \qquad (13)$$

Solution of this equation requires that constitutive equations relating ϵ and k to p_s be available. Shirato et al. (1970) used an equation similar to Eq. 13 to develop numerical solutions for sedimentation. Kos (1977) used a modified form of the Darcy

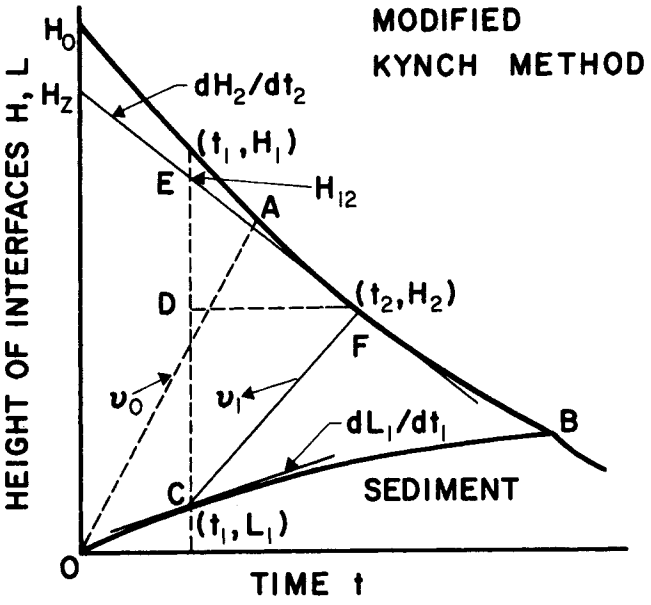

Figure 3. Modified Kynch method.

equation in which the structure of the cake and the essential parameters are assumed to be a function of the relative velocity as well as the effective pressure thus leading to a different equation.

SEDIMENT-SUSPENSION PROBLEM

Assuming that necessary parameters were available, the solution of the sediment-suspension problem depends upon the simultaneous solution of the first-order partial differential equation (Eq. 3) and the nonlinear second-order partial differential equation (Eq. 13) subject to the appropriate boundary conditions.

Solution of the sedimentation portion of the problem can be accomplished by the method of characteristics as dictated by Eqs. 4 and 5. In contrast to the Kynch procedure, each characteristic has its origin in the surface of the sediment which changes with time. To solve the analytical problem, the rate at which liquid is squeezed out of the sediment must be determined. Then with the upward velocity of the liquid known, the corresponding suspension concentration at the interface can be found through the concentration vs. sedimentation velocity relationship (Figure 2). The solids flux and the rate of sediment buildup must then be interrelated. With conditions fixed at the interface, the concentration rays or characteristics provide lines of constant composition which can be projected into the suspension. A material balance then yields the level of the descending supernatant layer.

COMBINING EXPERIMENT AND THEORY

It is instructive to develop a graphical interpretation of the equations as proposed in this article in order to compare the recommended changes with the original Kynch method. Figure 3 provides a picture of a sedimentation process in which the upper interface descends along H_oAFB while the sediment rises along OCB. The two interfaces meet at B, and the pure consolidation period of the sediment begins at that point.

When the sediment first forms at 0 ($t = 0$), a characteristic line along which a concentration wave with velocity $v_o = [d(u_s\phi_s)/d\phi_s]_{t=0}$ leaves the origin and travels toward point A which is the end of the constant rate period. Region OAH_o is characterized by a constant slurry concentration which is unaffected by the rising sediment. The first order partial differential equation (Eq. 3) controls that region.

Region OAB requires the simultaneous use of Eqs. 3 and 13. Past point B, the second-order, nonlinear partial differential Eq. 13 controls the solution.

Region OAH_o has a trivial solution, and we go directly to the first falling rate region and consider an arbitrary point C on the L vs. t curve. The concentration directly above C at $t = t_1$ is ϕ_{s1} which is also illustrated in Figure 4. A concentration wave with velocity v_1 as obtained from Figure 2C moves through the suspension and reaches the descending surface at H_2 as shown in both Figures 3 and 4. We assume that the slope dH_2/dt of the curve at H_2 corresponds to the velocity as given in Figure 2A for concentration $\phi_{s1} = \phi_{s2}$.

Use of experimental data as shown in Figure 3 implies that we have a solution to the partial differential equations (Eqs. 3 and 13) and have matched the boundary conditions at the interface. In particular we seek conditions relating the values of L and H and their derivatives to the basic parameters. We should like to provide a method which will yield the sediment velocity vs. concentration curve as accomplished in the Kynch method. Looking at Figure 3, we locate point H_2 and draw a tangent to its intersection of the H axis at H_z. Then the Kynch method states that

$$\phi_{s2} = \phi_{so}H_o/H_z \tag{14}$$

$$u_{s2} = dH_2/dt \tag{15}$$

We shall not find such a simple relation to be valid, but we shall develop an alternative expression. Our task revolves around determining the solids in the sediment and the boundary conditions at (t_1, L_1) as related to the point (t_2, H_2).

VOLUME OF SOLIDS IN SEDIMENT

At time t_1, the solids are divided between the sediment in (O, L_1) and the suspension (L_1, H_1) as follows:

$$\text{Volume in Sediment} = \int_o^{L_1} \epsilon_s dx \tag{16}$$

$$\text{Volume in Suspension} = \int_{L_1}^{H_1} \phi_s dx \tag{17}$$

All of the solids in L_1H_1 will cross the characteristic constant concentration ray $CF(L_1H_2)$ shown in Figures 3 and 4. The concentration and flux across L_1H_2 are both constant. The rate of flow of solids across L_1H_2 multiplied by the time $(t_2 - t_1)$ yields the total quantity of solids in L_1H_1 and permits us to calculate the values of the integrals in Eqs. 16 and 17. The ray goes upward

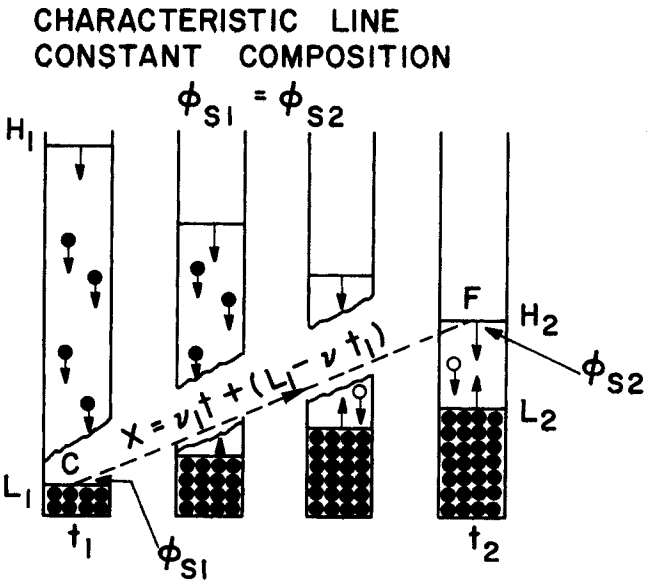

Figure 4. Characteristic line of constant composition.

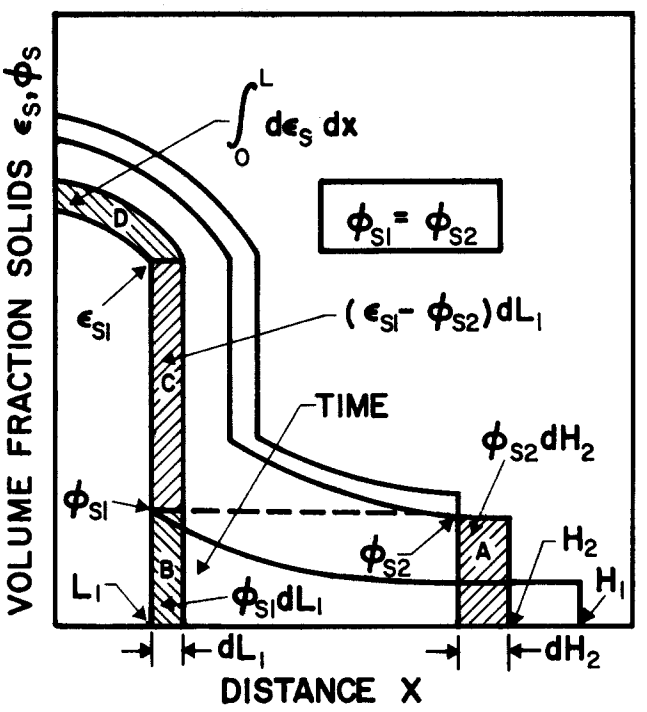

Figure 5. Volume fraction of solids vs. distance.

with velocity v_1 and the solids settle with velocity $u_{s2} = dH_2/dt$. The relative velocity with which the solids cross L_1H_2 is $-(v_1 - u_{s2})$ and the relative flux is $-\phi_{s2}(v_1 - u_{s2})$. The time is given by

$$t_2 - t_1 = \frac{H_2 - L_1}{v_1} \tag{18}$$

The solids in the sediment are given by

$$\int_0^{L_1} \epsilon_s dx = \phi_{s0}H_0 - \int_{L_1}^{H_1} \phi_s dx \tag{19}$$

$$= \phi_{s0}H_0 - \phi_{s2}\left(v_1 - \frac{dH_2}{dt}\right)(t_2 - t_1) \tag{20}$$

We now interpret Eq. 20 geometrically. The quantity $v_1(t_2 - t_1) = \overline{H_2 - L_1}$ or $\overline{CD}$ in Figure 3. The quantity $-(dH/dt_2)(t_2 - t_1) = \overline{DE}$. Consequently, the volume of solids in $(H_1 - L_1)$ is given by $\phi_{s2}(H_{12} - L_1)$ where H_{12} corresponds to point E, thus

$$\int_0^{L_1} \epsilon_s dx = \phi_{s0}H_0 - \phi_{s2}(H_{12} - L_1) \tag{21}$$

The Kynch method requires that $L_1 = 0$ which then leads to $H_{12} = H_z$.

Unfortunately, we can only use Eq. 12 if we already have the flux curve. Given dH_2/dt we could obtain ϕ_{s2} from Figure 2A and v_1 from Figure 2C. We could then verify whether or not the data fit the equations as derived. In addition, the procedure requires that no characteristics cross and that they be straight. If the characteristics cross, lines of constant composition will no longer be straight and must in general be found by numerical methods. The relative flux crossing a constant composition line would remain $-\phi_{s2}(v - dH_2/dt)$. However, v would not be a constant; and an integration would be required to give the total flux which is needed to calculate the volume of solids in the sediment. An average v can be defined so that the equation as presented can be used. The problem becomes more complicated.

We next turn to the boundary conditions at the sediment interface to see if additional information can be obtained from the slopes dH_2/dt and dL_1/dt_1.

SOLIDS FLUX AT SEDIMENT INTERFACE

The total solid volume in distance $0 - x$ where $L_1 \le x \le H_1$ is given by

$$\text{Volume of Solids} = \int_0^{L_1} \epsilon_s dx + \int_{L_1}^{x} \phi_s dx \tag{22}$$

Differentiating this expression yields a positive quantity which is the negative of the flux/area, q_s. As ϵ_s and ϕ_s are functions of (x, t) and L_1 is a function of t, differentiation produces

$$-q_s = \int_0^{L_1} \frac{\partial \epsilon_s}{\partial t} dx + (\epsilon_{s1} - \phi_{s1})\frac{dL_1}{dt} + \int_{L_1}^{x} \frac{\partial \phi_s}{\partial t} dx \tag{23}$$

Letting $x \to L_1^+$ yields the jump boundary condition (d'Avila and Sampaio, 1976)

$$q_s(L_1^+) = \int_0^{L_1} \frac{\partial \epsilon_s}{\partial t} dx + (\epsilon_{s1} - \phi_{s1})\frac{dL_1}{dt} \tag{24}$$

This represents the downward rate of transport of solids to the surface and equals $-\phi_{s2}dH_2/dt_2$. A graphical interpretation of Eq. 24 is given in Figure 5. The volume fraction of solids is plotted against x for L_1, $L_1 + dL_1$, H_2, and $H_2 + dH_2$. Conditions for points 1 and 2 are such that a horizontal line connects the two points so that $\phi_{s1} = \phi_{s2}$. Dropping the dt's, we see that $\phi_{s2}dH_2$ is given by area A; $\phi_{s2}dL_1$ by B; $(\epsilon_{s1} - \phi_{s1})dL_1$ by C; and the integral by area D. Subscripts have been placed on the t's to emphasize the difference between t_1 and t_2.

A physical interpretation of the various terms in Eqs. 22-24 follows:

Phenomenon	Area	Formula
Downward Flux	A	$-\phi_{s2}dH_2/dt_2$
Solid Flux Added to Sediment	$A + B$	$-\phi_{s2}\frac{dH_2}{dt_2} + \phi_{s1}\frac{dL_1}{dt_1}$
Same	$B + C + D$	$\epsilon_{s1}\frac{dL_1}{dt_1} + \int_0^{L_1} \frac{\partial \epsilon_s}{\partial t} dx$

Equating $A + B$ to $B + C + D$ or the equivalent A to $C + D$ yields

$$-\phi_{s2}\left(\frac{dH_2}{dt_2} - \frac{dL_1}{dt_1}\right) = \int_0^{L_1} \frac{\partial \epsilon_s}{\partial t} dx + \epsilon_{s1}\frac{dL_1}{dt_1} \tag{25}$$

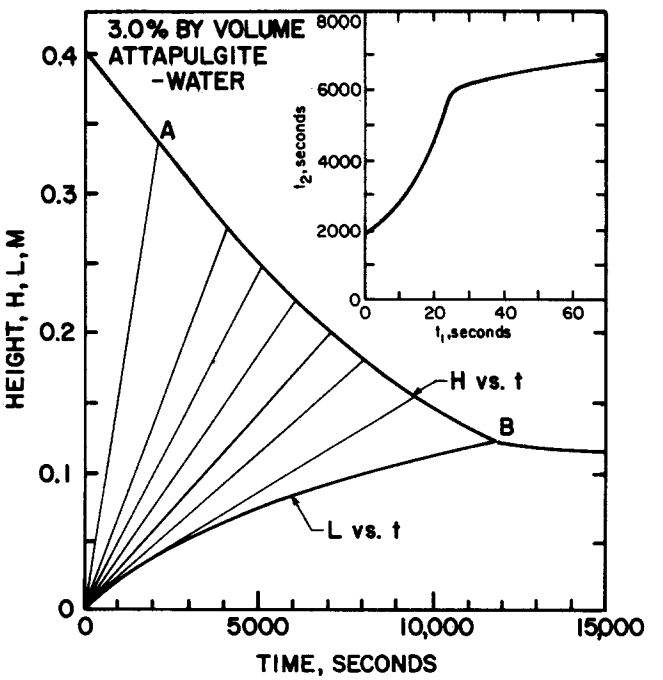

Figure 6. Height vs. time for attapulgite.

where ϕ_{s1} has been replaced by ϕ_{s2}.

We can also equate the left hand side of Eq. 25 to the derivative of Eq. 21 to obtain

$$\frac{d}{dt_1}\left[\phi_{s2}(H_{12} - L_1)\right] = \phi_{s2}\left(\frac{dH_2}{dt_2} - \frac{dL_1}{dt_1}\right) \tag{26}$$

Integrating this expression and substituting limits yields

$$\phi_{s0}H_0 - \phi_{s2}(H_{12} - L_1) = -\int_0^{t_1} \phi_{s2}\left(\frac{dH_2}{dt_2} - \frac{dL_1}{dt_1}\right)dt_1 \tag{27}$$

If we place $L_1 = 0$ and $H_{12} = H_z$, Eq. 27 reduces to the Kynch equation. Time t_2 becomes simply t, and $t_1 \equiv 0$. Thus the integral disappears.

Equation 26 can also be placed in the form

$$-\frac{d\phi_{s2}}{\phi_{s2}} = \frac{d(H_{12} - L_1)}{H_{12} - L_1} - \frac{dH_2/dt_2 - dL_1/dt_1}{H_{12} - L_1} \tag{28}$$

Integration produces

$$\phi_{s2} = \frac{\phi_{s0}H_1}{H_{12} - L_1}\, e^{\int_0^{t_1} \frac{dH_2/dt_2 - dL_1/dt_1}{H_{12} - L_1}\, dt_1} \tag{29}$$

If $L_1 = 0$, all of the characteristics will emanate from the origin; and t_1 will be zero. Thus the integral in the exponent in Eq. 29 approaches zero; and the equation coincides with Kynch's formulation. For L_1 to be zero, the cake must become infinitely dense; and the space occupied by the sediment must be replaced by a suspension which carries the correct characteristic signals to the descending interface. In spite of these theoretical deficiencies in the Kynch procedure, historically industry has been able to use it with success. Therefore it must represent some sort of reasonable approximation of the real case.

EXPERIMENTAL

Although many authors have published data involving the descending upper interface, very little information is available for growth of sediments. Data for sedimentation of attapulgite are shown in Figures 2 and 6. Settling velocities are somewhat scattered in Figure 2A, and the curve drawn through the data must be considered as an approximation. The average deviation for the 14 points shown is about $3.0(10^{-6})$ m/s. The characteristic velocity ν obtained as the slope of the flux curve in Figure 2B is particularly susceptible to variation in magnitude.

In Figure 6, descending and ascending interfaces are shown for a 3.0% by volume of attapulgite in water. The suspension originally had a height of 0.4 m. The constant rate period was considered to have ended at A (0.34 m, 2000 s), and the first falling rate period ended at B (0.125 m, 11,800 s). The 3% suspension falls in the region of maximum rate of change of the flux curve and provides a severe test for Eq. 29.

Numerical solutions of Eq. 29 were obtained by choosing a series of ν's that forced the *RHS* to equal ϕ_{s2}. The procedure consisted of the following:

1. A series of points were chosen on the H vs. t curve, i.e., points 1, 2, 3, 4. Point 2 is at (0.275 m, 4000 s).
2. The slope dH_2/dt_2 was found.
3. The corresponding concentration ϕ_{s2} was obtained from Figure 2A.
4. A series of tentative characteristic lines were drawn from each point until they intersected with the L vs. t curve at (L_1, t_1).
5. The slopes dL_1/dt_1 were found for each point (L_1, t_1).
6. Vertical lines were drawn from the tentative values of (L_1, t_1) so that H_{12} could be obtained in accord with the construction illustrated in Figure 3.
7. Values of (L_1, t_1) were chosen for each (L_2, t_2) so that the equality in Eq. 29 was satisfied.
8. The characteristic velocity was calculated from the slope $(L_2 - L_1)/(t_2 - t_1)$.

A few values of the characteristic slopes are shown as black dots on Figure 2C. Although the general trend is confirmed, additional data are needed for a variety of systems in order to more vigorously test Eq. 29.

ACKNOWLEDGMENT

The author wishes to express his appreciation to the National Science Foundation and the Conselho Nacional de Pesquisa of Brazil for support which enabled this work to be done while visiting COPPE (Coordenação de Programas Pos-Gradudados de Engenharia) of the Universidade Federal do Rio de Janeiro and the Universidade Federal de Sergipe. The author thanks J. S. d'Avila and Rubens Sampaio for their advice and cooperation. Sedimentation data were obtained as part of an undergraduate research project by John Wright, now of Geosources, Inc. Attapulgite used in the experiments was furnished by James Liner of Milwhite.

Mompei Shirato of Nagoya University corrected an error in the original manuscript involving Eq. 25. Terry Owens and Carla Tanberg assisted with calculations involving Figure 6. Bryant Fitch made many helpful suggestions.

NOTATION

g = acceleration of gravity, m/s^2
h = function of t
H = height of descending interface, m
H_o = initial value of H at $t = 0$, m
H_1, H_2 = values of H at t_1 and t_2, m
H_{12} = height defined on Figure 3, m
H_z = intercept of tangent to H curve on ordinate, m
k = permeability, m^2
L = height of sediment, m
L_1 = value of L at t_1, m
p_s = effective pressure, Pa
q = superficial velocity of liquid, m/s
q_s = superficial velocity of solids, m/s
t = time, s
t_1, t_2 = values of t at intersection of characteristic with sediment (t_1) and upper interface, t_2, s
u = average velocity of liquid, m/s
u_s = average velocity of settling solids, m/s
u_{s1} = value of u_s at sediment interface at t_1, m/s
u_{s2} = value of u_s at upper interface at t_2, m/s

Greek Letters

ϵ = volume fraction of voids in sediment, dimensionless
ϵ_s = volume fraction of solids in sediment, dimensionless
ϵ_{s1} = value of ϵ_s at cake surface at t_1, dimensionless
μ = viscosity, Pa · s
ν = characteristic velocity, m/s
ν_1 = characteristic velocity at t_1, m/s
ρ = density of liquid, kg/m^3
ρ_s = density of solid, kg/m^3
$\Delta\rho$ = $\rho_s - \rho$, kg/m^3
ϕ = volume fraction of liquid in suspension, dimensionless
ϕ_s = volume fraction of solids in suspension, dimensionless
ϕ_{s0} = initial suspension concentration, dimensionless
ϕ_{s1}, ϕ_{s2} = values of ϕ_s at sediment interface at t_1 and at upper interface at t_2, dimensionless

LITERATURE CITED

Aris, R. and N. R. Amundson, *Math. Meth. in Chem. Eng.*, "Vol. 2: First-Order Partial Differential Equations with Applications," p. 232-244, Prentice-Hall, Englewood Cliffs, NJ (1973).

d'Avila, J. S. and R. Sampaio, *Algumas considerações sobre o problema da sedimentação*, VII Encontro Sobre Escoamento em Meios Porosos, Rio Clara, SP, COPPE, Caixa Postal 1191, ZC-00, 20.000 Rio de Janeiro, RJ, Brazil (1979).

d'Avila, J. S. and R. Sampaio, *Condições de salto na sedimentação*, IV Encontro Sobre Escoamento em Meios Porosos, Jaboticabal, SP, COPPE, Caixa Postal 1191, ZC-00, 20.000 Rio de Janeiro, RJ, Brazil (1976).

Coe, H. S. and G. H. Clevenger, "Methods for Determining the Capacities of Slime-Settling Tanks," *Trans.*, Amer. Inst. Min. Engrs., **60**, 356-384 (1916).

Fitch, E. B., "Current Theory and Thickener Design," *Ind. Eng. Chem.*, **57**, 19-25 (1965).

Fitch, E. B., "Current Theory and Thickener Design, Parts 1, 2, 3," *Filtration and Separation*, **12**, 355-359; 480-488, 553, 636-638 (1975).
Kos, P., "Fundamentals of Gravity Thickening," *Chem. Eng. Prog.*, **73**, 99-105 (1977).
Kynch, G. J., "A Theory of Sedimentation," *Trans.*, Faraday Soc., **48**, 166-176 (1952).
Scott, K. J., "Mathematical Models of Mechanism of Thickening," *IEC Fundamentals*, **5**, 109-113 (1966).
Scott, K. J., "Thickening of Calcium Carbonate Slurries," *IEC Fundamentals*, **7**, 484-490 (1968).
Scott, K. J. and J. L. Alderton, "Maximum Solids Handling Capacity of Continuous Thickeners," *Trans.*, Instn. Min. Metall., **75C**, 201-210 (1966).
Shirato, M., H. Kato, K. Kobyashi, and H. Sakazaki, "Analysis of Settling of Thick Slurries Due to Consolidation," *J. Chem. Eng.*, Japan, **3**, 98-104 (1970).
Talmadge, W. P. and E. B. Fitch, "Determining Thickener Unit Areas," *Ind. Eng. Chem.*, **47**, 38-41 (1955).

Manuscript received December 11, 1979; revision received November 21, and accepted December 10, 1980.

Characterization and Analysis of Continuous Recycle Systems:

Part II. Cascade

UZI MANN

Department of Chemical Engineering
Texas Tech University
Lubbock, Texas 79409

and

MICHAEL RUBINOVITCH

Faculty of Industrial Engineering and Management
Technion-Israel Institute of Technology
Haifa, Israel

A general analysis of a cascade of identical recycle units is presented by means of studying the fluid history inside the system. This is an extension of Part I (Mann et al., 1979) in which a single recycle unit was analyzed. The history of a fluid element is expressed in terms of the number of cycles it completes, the time it resides in the system and the total time it resides in a specific section of the system—all are random variables. Concepts from probability theory and stochastic processes are used to derive the number of cycles distribution (NCD), residence time distribution (RTD) and various total regional residence time distributions (TRRTDs) as well as their means and variances. Expressions for the joint distributions of pairs of these random variables are also derived as well as explicit expressions for their covariances and correlation coefficients. Two applications of the results are illustrated: one in analyzing a continuous spouted-bed coating unit and the second in using the cascade as a flexible, physically based multi-parameter flow model.

SCOPE

The history of a fluid element (or particle) in a continuous recycle system is characterized in terms of the number of cycles it completes, the time it resides in the system and the total time it resides in specific regions of the system. Detailed information on particle history can be quantitatively expressed by the joint distributions of pairs of these characteristics, by the number of cycle distribution (NCD), the residence time distribution (RTD), and the total regional residence time distribution (TRRTD). Joint distributions, their covariances and correlating coefficients are useful in analyzing processes in which particles undergo changes according to two different mechanisms (e.g., reaction and attrition of coal particles in a gasification unit).

The NCD is useful in analyzing processes in which the quality of the product is related on the number of cycles a particle completes (e.g., spouted bed coating). The RTD is useful when the quality of the product depends on the residence time in the system (e.g., chemical reaction) and in formulating flow models. The TRRTD is useful when particles undergo changes in certain sections of the system (e.g., reaction occurring in a high-temperature region).

In Part I (Mann et al., 1979) these concepts were introduced and a single recycle unit was studied. Explicit expressions for the joint distribution of the number of cycles and residence time, the NCD, RTD, TRRTD as well as the covariances and correlation coefficients of pairs of these characteristics were derived. In this article the analysis is expanded to a cascade of identical recycle units connected in series.

Part I of this paper appeared in *AIChE J.*, **25**, 873 (1979).

0001-1541-81-4870-0829-$2.00.